LABORATÓRIO DE INSTRUMENTAÇÃO E
FÍSICA EXPERIMENTAL DE PARTÍCULAS

LIP / 01–01

January 2001

EGS4 and MCNP4b MC Simulation of a Siemens KD2 Accelerator in 6 MV Photon Mode

A Chaves♮, C Alves♮, M Fragoso¶[1], M C Lopes♮, C Oliveira§, L Peralta¶[2], P Rodrigues¶, J Seco¶[3] and A Trindade¶

♮ CROC, Centro Regional de Oncologia de Coimbra do IPOFG, Av.Bissaya Barreto, 3000-075 Coimbra, Portugal

§ ITN, Instituto Tecnológico e Nuclear, Estrada Nacional 10, 2685-953 Sacavém, Portugal

¶ LIP, Lab. Instr. Fis. Exp. Part. and FCUL, Fac. Ciencias Univ. Lisboa Av. Elias Garcia, 14-1, 1000-149 Lisboa, Portugal

Abstract

The geometry of a Siemens Mevatron KD2 linear accelerator in 6 MV photon mode was modeled with EGS4 and MCNP4b. Energy spectra and other phase space distributions have been extensively compared in different plans along the beam line. The differences found have been evaluated both qualitative and quantitatively. The final aim was that both codes, running in different operating systems and with a common set of simulation conditions, met the requirement of fitting the experimental depth dose curves and dose profiles, measured in water for different field sizes. Whereas depth dose calculations are in a certain extent insensible to some simulation parameters like electron nominal energy, dose profiles have revealed to be a much better indicator to appreciate that feature. Fine energy tuning has been tried and the best fit was obtained for a nominal electron energy of 6.15 MeV.

[1]Presently at Physics Department, The Royal Marsden NHS Trust, London, UK.
[2]luis@lip.pt
[3]Presently at Joint Department of Physics, Institute of Cancer Research and Royal Marsden NHS Trust, Sutton, UK.

1 Introduction

Medical physics, in general, and radiotherapy in particular, are nowadays privileged application fields for Monte Carlo (MC) simulation. In the last two decades, the number of published papers on the subject has become an undeniable indication of this interest (Mackie *et al* 1990, Andreo 1991, Rogers *et al* 1995, Ma *et al* 1997). In fact, the continuous development undergone by the technology of radiation production machines, associated with systematic approaches into radiobiology, are dictating and requiring more and more precision and accuracy in dose prescription and delivering in order to reach expected outcomes in tumour control free of complications (Aaltonen *et al* 1996, ICRU 1993, ICRU 1999). These highly demanding requirements are the basis for the need of a powerful analysis tool that accounts for all aspects of primary and secondary radiation transport inside the treatment machine head, and also within the patient. Monte Carlo simulation is, by definition, that kind of approach. MC techniques are suitable to study difficult radiation transport problems as much as simple energy degradation processes.

Monte Carlo based treatment planning systems (TPS) can already be previewed as the future basis for 3D dose distribution in clinical calculations (Ma *et al* 1999, Patterson *et al* 2000). Meanwhile, MC in-house solutions, based on parallel processing techniques that distribute the calculations throughout some sort of local network of personal computers, will probably serve as a local alternative analysis tool for clinical comparisons with conventional TPS, in some problematic cases (Faddegon *et al* 1998, Solberg *et al* 1998, DeMarco *et al* 1998, Sanchez-Doblado *et al* 2000). In order for this ideal future to become truth in the routine clinical practice, a great deal of efforts still have to be put on exhaustive studies involving intercomparisons between different MC codes. Whenever it is possible, experimental validation of these MC results constitute an accurate and reliable calculation basis for further development into clinical situations (Libby *et al* 1999). Following some authors (Siebers *et al* 1999) it is thus convenient to consider two separate components in the overall radiotherapy simulation process: i) the patient-independent (beam line) MC simulation and ii) the treatment planning MC simulation. In this paper we will be devoted to the first issue, simulating a linear accelerator head (Siemens Mevatron KD2) in 6 MV photon mode, with two different MC codes: EGS4 (Nelson *et al* 1985) and MCNP4b (Briemeister 1997). The treatment simulation is capable of providing details of the clinical beam far beyond any experimental technique (Faddegon *et al* 1998). The resulting beam representations are compared at different distances from the source, along the beam line components (target, flattening filter, ionization chamber, etc). It is instructive to compare independent calculations of phase space distribution (PSD) parameters, despite the fact that the extremely high intensity of therapeutic photon beams makes the direct measurement of energy spectra practically impossible and no measured angular distribution data is available on literature (Mohan *et al* 1985), except some magnetic spectrometer measurements considered as complementary to Monte Carlo calculations (Deasy *et al* 1996). It is necessary to be familiar with the capabilities and limitations of each code to evaluate if the different physical

models and algorithms used lead to significantly different results at the PSD level, and whether these differences are reflected in dose calculations. With this concern, some effort has been put on experimental dose determinations, using different ionization chambers (with sensible volumes ranging from 0.015 cm^3 to 0.300 cm^3) and different measurement set-ups (chamber axis parallel and orthogonal to the beam axis) in order to appreciate the different integral response in the beam profile edges (high dose gradient regions) and correlate these differences with the geometry of the scoring cells used in MC calculations.

Historically, both codes (or their precursors) have had different origins: EGS4 was initially developed to simulate high-energy electromagnetic cascades, up to several thousands of GeV, whereas MCNP4b (or ETRAN and ITS) started from the low energy side, up to a few MeV (applied to nuclear reactor physics). Comprehensively, the weaknesses revealed by both codes, when dealing with radiotherapy applications (Andreo 1991, Rogers and Bielajew 1986), derived from this opposite energetic origin. Nevertheless, the evolution encompassed by both codes, through systematic approaches on dealing with the basic physical processes (secondary electron production, multiple scattering, bremsstrahlung production) as much as on refined cross-section data, on modelling methodologies and algorithms (random number generators, electron energy indexing, geometrical packages, variance reduction techniques) has progressively reduced the differences (Siebers *et al* 1999, Love *et al* 1998, Jeraj *et al* 1999). In order to reach a common basis for further developments for patient dependent simulations, and assuming that both EGS4 and MCNP4b are equally suitable for the generation of phase space distributions, we mainly focused on establishing the same set of simulation conditions: energy cut-offs, geometry simplifications, number of scoring cells, etc. With this common basis and the inherent qualitative and quantitative differences in phase-space distributions along the beam line, the final aim was that both codes (running in different operating systems) met the requirement of fitting experimental depth dose curves and dose profiles measured in water.

2 Materials and Methods

The geometry of the Siemens KD2, in 6 MV photon mode, was modelled both in EGS4 and MCNP4b. For MCNP4b the combinatory geometry package was used. For EGS4 the accelerator head was modelled using an in-house geometry package developed for that purpose. Detail technical construction data was kindly provided by Siemens AG Medical Engineering. A schematic view of the accelerator head in photon mode is displayed in figure 1. Standard elements of the accelerator head were grouped in three main modules: target (including the beam stopper), flattening filter (with primary collimator) and the secondary collimator (plus ionization chamber and mirror). At the end of each module the relevant information of the particles was stored in phase space data files. Two radiation field sizes, 5×5 cm^2 and 10×10 cm^2, at 100 cm Source-to-Surface Distance (SSD) were considered on a water phantom with dimensions $50 \times$

50×50 cm^3. The PSD after module 3 was used to obtain the MC calculated percent depth dose (PDD) and dose profile curves, which were compared to the experimental data.

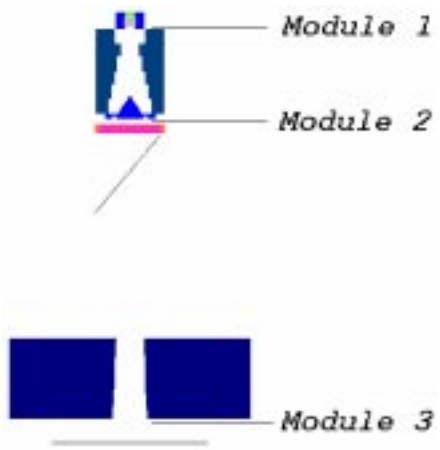

Figure 1: Schematic view of a Siemens KD2 accelerator in 6 MV photon mode (outer jaws not shown)

2.1 EGS4 Simulation

The EGS4 Code system leaves the user the problem of coding the geometry except for trivial geometrical setups. The problem might be a rather difficult one when the user is interested in complex geometries. In the past, several user codes were developed, with the primary aim of simulating electron and high-energy photon beams from clinical accelerators (Rogers *et al* 1995, Udale 1988, Lovelock *et al* 1995). A somehow different approach was implemented for geometry coding, where a set of user routines were developed and tested over several years, and assembled in the in-house User Code. One of the main features is the coding possibility of complex geometries, through the use of simple geometric shapes. The available shapes include boxes, cylinders, rings, spheres, cones and a general trapezoid, that can be tilted relatively to one of the axis. When tracking a particle across the boundary of a geometrical shape, the program will only search for the new geometrical region between the first neighbours. This strategy speeds up the program and allows rather complex geometries to be implemented sparing time in the localization of the particle (Fragoso *et al* 1999).

This User Code relies in some auxiliary packages from the CERNLIB Program Library (1996). This allowed the implementation of a highly robust user code for I/O operations, with advanced data analysis options and upgraded random number generators.

Run-time histograming is achieved with HBOOK package (Brun 1994),

where events can be scored in one-and two-dimension histograms at run-time, at areas of the geometrical setup (with conditions of booking being previously defined by the user). HBOOK also includes a general histograming structure called *Ntuples* (Brun 1994), which is a general data structure where variables, namely position, energy, direction cosines, characterizing one event are stored in columns and each event is placed in a row. These structures allow for a very flexible way to analyse data with PAW package (Brun *et al* 2000) from CERNLIB. Furthermore, due to their binary format a gain in space storage is achieved.

In EGS4 (version 3.2) the RANMAR random number generator was replaced by the RANLUX generator (Lüsher 1994) as available in the CERNLIB distribution (James 1994). Different quality or luxury levels are available, with a trade-off in speed. In this work, the default quality level (3) was used. Simulations were run in parallel on five Digital Alpha Workstations, where for each workstation different initial sequences were assigned, in order to guarantee the statistical independence of the results.

The incident electron beam was assumed to be monoenergetic point-like, with a kinetic energy of 6 MeV. The total electron energy cut-off (ECUT) was set to 700 keV and the photon energy cut-off (PCUT) was set to 10 keV. Secondary particle production thresholds were set to 521 keV for charged particles (AE), and 10 keV for photons (AP). Water phantom dose calculations were performed with the same energy cut-off and secondary particle production thresholds. These values were chosen after preliminary runs and based on the work of other authors (Rogers *et al* 1995, Siebers *et al* 1999, Deng *et al* 2000). The PRESTA algorithm (Bielajew and Rogers 1987) was used with a maximum fractional energy loss per electron step, due to continuous processes (ESTEPE) of 1%. This value was considered to be a compromise between simulation time and correct electron backscattering simulation, especially for high-Z materials (Jeraj *et al*). The material databases used include both the density and bremsstrahlung corrections recommended by ICRU *Report* 37 (1984).

For the first module, a total of 10^8 incident electron histories were simulated. For the second and third modules, the number of simulated histories varied from 2×10^7 to 5×10^7. When the number of particle histories to be simulated exceeded the number of particle histories stored, a re-sampling was performed. No variance-reduction techniques were employed.

2.2 MCNP4b Simulation

MCNP4b is a continuous energy, generalized geometry, time dependent, coupled or de-coupled neutron-photon-electron Monte Carlo code. For photons and electrons transport the energy range goes from 1 keV to 1 GeV. MCNP4b reads information from an input file, which allows the user to specify: the geometry and materials, cross sections, particles to be transported (neutrons, photons and electrons), radiation source specifications, types of tallies to be obtained, variance reduction techniques to improve the efficiency and physics parameters. The standard geometrical cell construction relies on Boolean combinations of

first and second degree surfaces and fourth degree elliptical tori. For each cell its relative importance, energy cut-off and material should be assigned by the user.

Two physic models are possible, the *simple* and the *detailed* one. The *simple* model is intended for high-energy photons where little coherent scattering occurs, but it is inadequate for high-Z nuclides. Due to this fact, the *detailed* model has been used. It includes coherent scattering and accounts for fluorescent photons after photoelectric absorption. Electron binding effects are also accounted by the inclusion of form factors.

A crucial question of the MCNP4b code is the generation process of the bremsstrahlung photons. In spite of some available information, some authors (Siebers *et al* 1999) advise against the use of the bremsstrahlung splitting. The problem consists in output photons, after the splitting, having identical phase space coordinates. As a consequence, the bremsstrahlung splitting has not been used (default input parameter BNUM = 1). The electron energy indexing algorithm used was the ITS-style with nearest group boundary treatment. The upper energy limit for the electron interactions (EMAX) was the default value, 100 MeV, for all the runs. This value was chosen since Siebers *et al* (1999) noticed some changes on bremsstrahlung photon production when using non-standard EMAX values.

A dedicated code, *mcnp_strip*, was used in order to directly compare the MCNP phase space distributions obtained at the end of each module (using the SSW card) with the equivalent distributions from EGS4. This code originates from the LAHET Monte Carlo code and was adapted to MCNP and improved by Siebers (2000). In analogy to the EGS4 User Code, a re-sampling was done everytime the number of simulated particles exceeds the number of independent histories. The photon splitting was used in water. For the plan upstream the second module 2.5×10^7 of independent histories have been obtained; for the plan upstream the third module 3.2×10^5 have been obtained (5×5 cm^2 field) or 1.2×10^6, (10×10 cm^2 field). Several approximations were studied in order to optimise the running time without changing significantly the results from a statistically point of view (Chaves *et al* 1998). These included the increase of electron and photon energy cut-offs to 700 keV (total energy) and 10 keV respectively, and geometry truncation of the primary collimator.

2.3 Experimental Data

The experimental data for the validation of the simulation results was obtained in a 3D motorized water phantom (MP3-PTW), with thimble type waterproof ionization chambers, whose geometrical characteristics are presented in Table 1. The standard chamber for relative dose measurements is a 0.125 cm^3 (PTW type 233642) sensitive volume. Other chambers, with different sensitive volumes (see Table 1), were also used in the high dose gradient region (the penumbra region in dose profile measurements), in order to understand the influence of the chamber dimensions on dose measurements: a 0.300 cm^3 (PTW type M31003) and a 0.015 cm^3 (pin-point chamber). The chambers were positioned in different

Table 1: Dimensions of the ionization chambers (see text)

Sensitive Volume (cm^3)	Length (mm)	Diameter (mm)
0.015	5.0	2.0
0.125	6.5	5.5
0.300	16.3	5.5

measurement setups: horizontal (with the longitudinal chamber axis perpendicular to the beam central axis) and vertical (with the longitudinal chamber axis parallel to the beam axis).

3 Results and Discussion

3.1 Accelerator Head Simulation

Data analysis, on EGS4 and MCNP4b *Ntuples* were performed, in order to characterize the initial photon beam produced at the target. The bremsstrahlung spectra and the average photon energy as function of the radius are presented in figures 2a and 2b. Photon spectra were normalised to its maximum value on the different planes. This procedure removes the integral bremsstrahlung production differences between EGS4 and MCNP4b, as suggested by Siebers *et al* (1999).

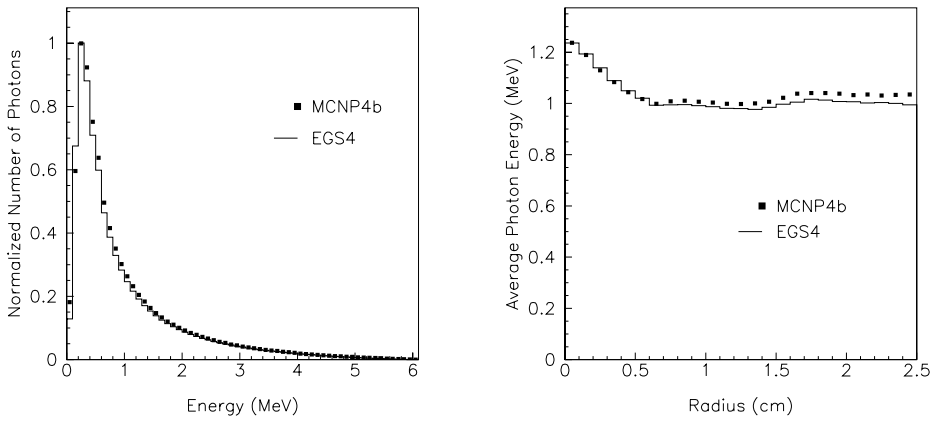

(a) (b)

Figure 2: At first module level: **a**) bremsstrahlung spectra and **b**) average photon energy as a function of scoring radius

The bremsstrahlung spectra were scored in a circle with 2.5 cm radius.

Statistic uncertainties are less than 1% for both codes and are therefore not shown. The total average photon energy for the EGS4 simulation is 0.972 MeV while for MCNP4b the average energy is to 0.989 MeV. When the scoring radius was reduced to 0.6 cm (only direct photons produced in the target, travelling at low-angles are scored) the average photon energies are 1.040 MeV and 1.044 MeV, for EGS4 and MCNP4b, respectively, denoting a very good agreement. Figure 2b shows that within the central region (radius $\leq$ 0.6 cm) the average energy values are similar for both codes but for larger radius, the average photon energy is higher in MCNP4b than in EGS4. The observed differences, within 25 to 50 keV, have statistical meaning since the errors for each bin are of the order of 5 keV for both codes. This differences obtained without radius restrictions can be related to an hardening process of photons exiting the target material with higher angles into the beam stopper in MCNP4b simulations.

An equivalent analysis for the flattening filter (second module) is present in figures 3a, 3b and 4. In general, the average photon energy as a function of scoring radius calculated by MCNP4b is slightly lower than the one calculated by EGS4 (see figure 3b). Statistic uncertities are less than 5 keV, while differences beteween EGS4 and MCNP4b results reach 50 keV. Total average photon energy for EGS4 and MCNP4b are 1.170 MeV and 1.156 MeV respectivey.

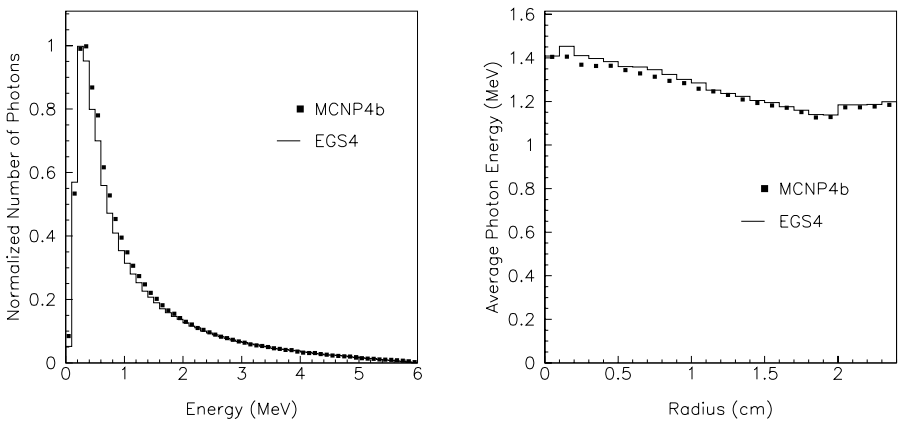

(a) (b)

Figure 3: Second module level: **a**) energy photon spectra and **b**) average photon energy as a function of scoring radius

When comparing the average photon energy at the end of the flattening filter (see figure 3b) with the corresponding value at the target level (see figure 2b), the hardening effect on the spectrum is evident. The average photon energy shows a monotonically decrease from the highest value 1.40 MeV at r = 0 cm to 1.15 MeV at r = 2 cm.

The second important effect of the flattening filter is illustrated on figure 4,

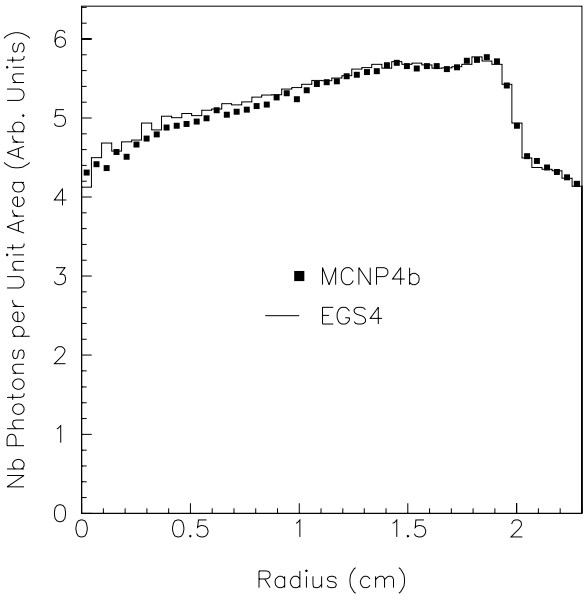

Figure 4: Simulated total number of photons per unit area as a function of the scoring radius the end of the second module

where the smoothed slope of number of photons per unit area is compensated by the inverse slope of figure 3b, leading to flat dose distributions in the water phantom.

Both simulations, EGS4 and MCNP4b, are in agreement, but the average energy values seem to be much lower than those reported for the 6 MV photon mode, although with different accelerators. In fact, reported average photon energies for 6 MV photon mode present a wide energy range, which should be related with different flattening filter geometries, different target materials (Chaney *et al* 1994) but also with different definitions of average energy. Indeed, there are different weighting functions used: fluence, dose and number of particles (Lee 1997). In this work the last option was used. Also, some authors report a *perceived value* of one-third of the maximum energy for the average value (Lewis *et al* 1999), following original work from LaRiviere (1989) but not always clearly defined. Indeed, according to LaRiviere the incident kinetic electron energy value relates with the dose-weighted average energy of the unflattened photon beam by:

$$E_d = 10^{0.998E-0.441} \tag{1}$$

where E_d is the dose-weighted average energy (in MeV) and E is the electron incident kinetic energy (in MeV), LaRiviere obtained also a good correspon-

dence between the percentage dose at 10 cm (PDD_{10}) and the dose-weighted average energy of the filtered beam:

$$E_d = 10^{(PDD_{10}-55.37)/28.68} \tag{2}$$

In order to compare our results with the calculated values obtained with (1) and (2), dose-weighted conversion factors for monoenergetic photon beams were obtained using EGS4. For this purpose, an uniform distribution from 10 keV to 6 MeV was used as the input spectra, and the corresponding dose at a 10 cm depth in water phantom was obtained. At the target level, bremsstrahlung photons along the central axis were selected, and the total number of photon distribution were converted to dose-weighted distributions, using the pre-calculated factors. The average value is 2.238 MeV and can be compared with the calculated value, for an incident beam of 6 MeV using equation (1) to be 2.172 MeV. This same kind of calculations are reported by Lee (1997) with similar results. EGS4 filtered spectrum, obtained at the plane immediately below the flattening filter present a dose-weighted average energy of 2.498 MeV. Experimental percentage dose at 10 cm depth for a Siemens KD2 in 6 MV photon mode is 66.7%, which according to equation (2) indicates a dose-weighted average energy of 2.480 MeV. This two values agree within 0.7%. This is an indication that our results are consistent with those predicted by other authors based on the work of LaRiviere.

At the third module level (after the secondary collimator) the phase-space distributions were calculated for 5×5 cm^2 and 10×10 cm^2 field sizes. In figures 5a and 5b photon spectra and average photon energy are presented for 10×10 cm^2 field size.

Discrepancies beteween EGS4 and MCNP4b are consistent with those shown previously. Total average photon energy for EGS4 is 1.688 MeV for and 1.684 MeV for MCNP4b. It should be noted that the average photon energy is approximately constant on the area limited by the jaws. This value is higher than the average photon energy obtained after the flattening filter. This is due to the fact that the secondary collimators, besides limiting the field, also discard photons with high polar angular values which correspond in average to those photons with lower energy.

3.2 Phantom and Dose Simulations

Final validation of phase space distributions were performed against experimental central axis depth doses and profiles at several depths, measured with the 0.125 cm^3 chamber. The scoring volume for depth doses was a cylinder, placed along the central axis, with a 6.5 mm radius and 6 mm height. Calculated depth dose curves by EGS4 and MCNP4b for 5×5 cm^2 and 10×10 cm^2 field sizes are shown in figure 6a and 6b respectively. Each set of simulated results were normalized to each maximum dose. Results agree with experimental values within 1-2%.

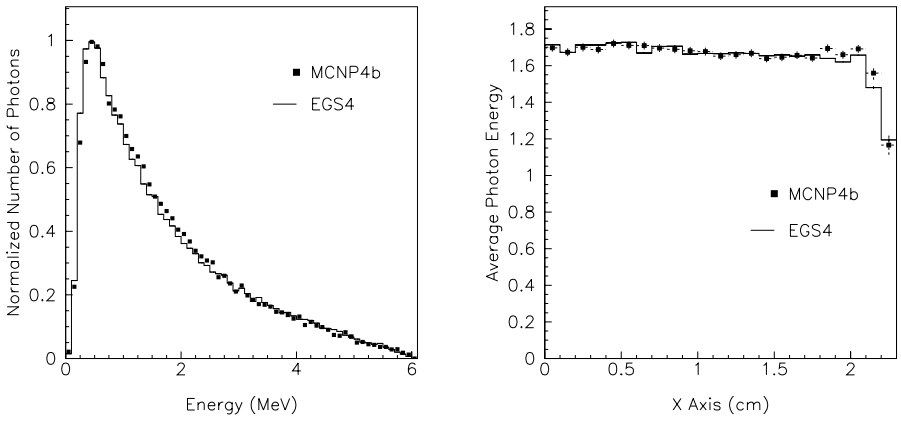

(a) (b)

Figure 5: Third module level for a 10×10 cm^2 field size: **a**) bremsstrahlung spectra and **b**) average photon energy as a function of scoring distance from central axis

Simulated lateral dose profiles where also compared with experimental data. At each depth, dose profiles were normalized to the central axis dose value. Scoring volume for dose profiles were assumed to be voxels with two typical dimensions: 7 mm (beam axis) $\times$ 2 cm (in-plane axis) $\times$ 6 mm (cross-plane axis) along the flat region of the profile, and 7 mm (beam axis) $\times$ 2 cm (in-plane axis) $\times$ 1 mm (cross-plane axis) in the penumbra region. Results are displayed in figures 7a and 7b for a 5 and 10 cm depth profiles along the cross-plane axis.

It is clear that both results of EGS4 and MCNP4b are different from experimental measures. There is a clear calculated over dosage creating the so called profile horns (Lovelock *et al* 1995). Assuming that these differences are due to the energy chosen for the initial electron beam, fine tuning was performed by changing the incident electron energy. Energy values between 5.58 and 6.3 MeV were tested. To reduce the CPU time involved in this process geometrical cuts were implemented. Particles reaching primary and secondary collimators were discarded. This allowed a gain of about 50% on simulation time, with the drawback of neglecting the electron contamination arising from the interaction of the photon beam with the primary and secondary collimators, and photon transmission itself from the secondary collimators. However electron contamination at this depths does not change significantly dose distributions (Li and Rogers 1994) and photon transmission from the secondary collimator will only affect penumbra regions outside the field edge, with less clinical relevance (Patterson *et al* 2000). Results for 6.15 MeV and 5.58 MeV nominal energy are showed in figures 8a and 8b for a 10×10 cm^2 field size. Starting from 5.58

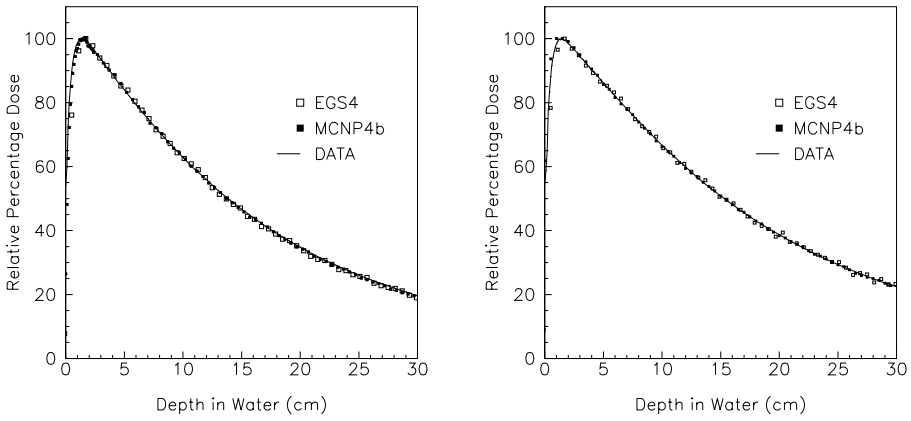

(a) (b)

Figure 6: Experimental and simulated depth dose curves for: **a**) 5×5 cm^2 field size **b**) 10×10 cm^2 field size

MeV, as the initial electron energy is increased to 6 MeV and then to 6.15 the profile plateau becomes more flat, and the adjustment to experimental data significantly improves for EGS4. To cross-check this value MCNP4b simulations were then run with full geometry description at 6.15 MeV The results are displayed in figure 8, indicating a good adjustment for the two codes, achieved with the same energy value. The effect of the fine tuning procedure on depth dose curves was also evaluated. Depth dose curves at 6.15 MeV differ from the 6 MeV simulations, by less than 1.5%. The dependence of dose profiles shape with initial electron energy can be regarded as an accurate indicator of the true accelerating potential (Libby *et al* 1999, Lovelock *et al* 1995), which for this particular accelerator is about 6.15 MeV.

The half dose profile curves at 5 cm depth for the 6.15 MeV case are showned for both codes in figure 9a. A maximum deviation of 2 mm is seen in profile penumbra for both MC codes

In figure 9b, truncated half-profiles measured at 5 cm depth for the 10×10 cm^2 field size are shown. Different curves correspond to different measurement setups, different chambers and different chamber orientations as described before. These kind of study is closely related with the dimension of the scoring cells chosen in Monte Carlo dose profile calculations. In fact, when we compare EGS4 and MCNP4b dose profile calculations with experimental results and errors in the order of 1 or 2 mm are mentioned in the penumbra region, it should also be explicitly mentioned that the scoring cells dimension in the scanning direction is similar to the ionization chamber diameter used for that comparison. Further conclusions can be drawn from figure 9b. As the transversal dimension

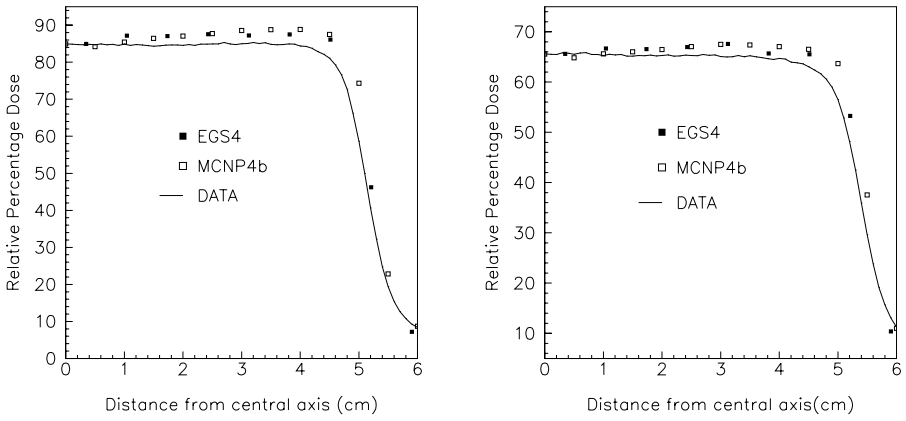

(a) (b)

Figure 7: Experimental and simulated truncated cross-plane dose profiles at 6 MeV nominal energy for 10×10 cm^2 field at: **a)** 5 cm depth and **b)** 10 cm depth

for the 0.300 cm^3 and 0.125 cm^3 chambers is the same and the profiles practically coincide, we can conclude that the different chamber length does not influence the relative measurement. This same conclusion is reinforced when we compare the curves corresponding to vertical and horizontal positioning of the 0.300 cm^3 chamber, and no significant differences are shown, because the scanning direction (in-plane) is orthogonal to the chamber length and the spatial resolution is just determined by the transversal dimension (diameter). The greater spatial resolution achieved with the pin-point chamber demonstrates that in high dose gradient regions, the dimension of the measuring detector is crucial to resolve those steep dose profiles and that errors of 1 mm can easily be made.

4 Conclusions

The Siemens Mevatron KD2 is one of the existing linear accelerators at the *Centro Reional de Oncologia de Coimbra*. This machine is not usually referenced in literature. Phase space distributions for this machine, mandatory for patient dose calculations are not commonly available. The detailed simulation of this accelerator with two different Monte Carlo codes, EGS4 and MCNP4b, is thus very interesting. EGS4 simulations were based on a in-house user code. This option offers some advantages, namely detailed geometry control, scoring and data analysis. Different phase space distributions were examined along the linear accelerator head. Differences between codes are small, supporting the

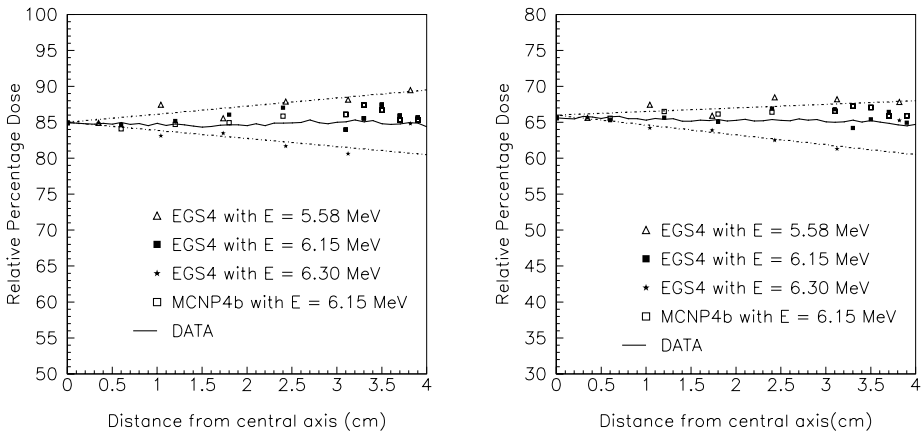

(a) (b)

Figure 8: Energy tuning results for the flat region of dose profiles for the 10×10 cm^2 field size at: **a)** depth dose curve and **b)** dose profile curve at 10 cm depth.

idea that EGS4 and MCPN4b are equal suitable for phase space data generation. This step by step intercomparison has enabled a tight control of the whole simulation process and constitutes a confidence support for subsequent studies. Simulated percentage depth dose values agree with experimental data within 1-2%, even if parameters like nominal electron energy were slightly changed. The beam was considered to be monoenergetic, although several percent energy dispersion is claimed by the manufacturer. This approximation is supported by the small sensitivity of depth dose curves to the exact energy value. The shape dependence of the dose profiles with initial kinetic energy of the electron beam can be regarded as a more accurate indicator of the true accelerating potential. Energy fine tuning was performed in order to obtain the best agreement between simulation dose profiles and experimental profiles. The best fit was obtained with an energy of 6.15 MeV for both MC codes, a value several percent higher than the manufacturer reported value.

5 Acknowledgments

The authors are grateful for the detail technical construction data kindly provided by Siemens AG Medical Engineering. We would also like to thank to Dr J V Siebers for enlightening discussions on some topics of this work. In addition, our thanks to Dr F Sanchez-Doblado, Dr T D Solberg and Dr F Verhaegen for a critical reading of the manuscript. This work was partially supported by FCT project CERN/P/FIS/15174/1999.

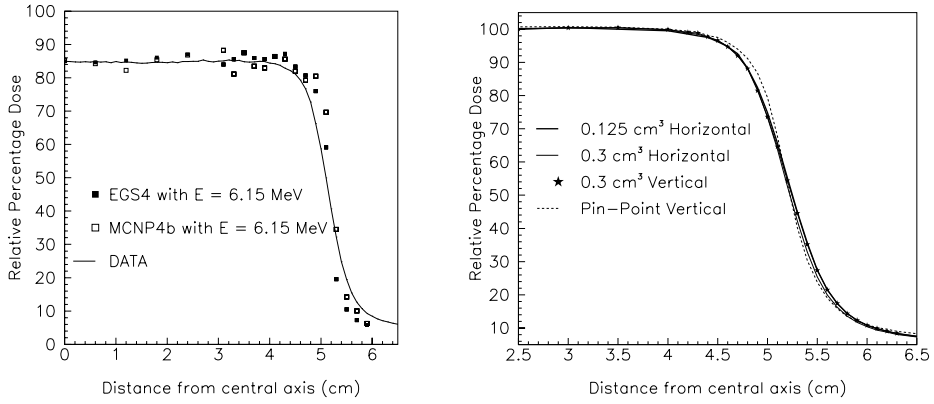

(a) (b)

Figure 9: Energy tuning results for the flat region of dose profiles for the 10×10 cm^2 field size at: **a)** 5 cm depth and **b)** half-profiles measured at 5 cm depth for the 10×10 cm^2 field size with different measurement setups

References

Aaltonen P, Brahme A, Lax I, Levernes S, Naslund I, Reitan J B and Turesson I 1996 Specification of dose delivery in radiation therapy *Acta Oncol.*, Suppl.10

Andreo P 1991 Monte Carlo techniques in medical radiation physics *Phys. Med. Biol.* **36** 861–920

Bielajew A F and Rogers D W O 1987 PRESTA: the parameter reduced electron-step transport algorithm for electron Monte Carlo transport *Nucl. Instrum. Methods* B **18** 165–81

Briemeister J F 1997 MCNP-general Monte Carlo N-particle transport code version 4b *Report* LA-12625-M (Los Alamos, NM: Los Alamos National Laboratory)

Brun R 1994 *HBOOK - Statistic Analysis and Histogramming* CERN Program Library Long Writeup Y250 (Geneva, Switzerland:European Organization for Nuclear Resarch)

Brun R, Couet O, Cremel N L, Vandomi C and Zanarini P 2000 *PAW - Physics Analysis Workstation* CERN Program Library Long Writeup Q121 (Geneva, Switzerland:European Organization for Nuclear Resarch)

CERNLIB 1996 *CERN Program Library Short Writeups*, (Geneva, Switzerland:European Organization for Nuclear Resarch)

Chaney E L, Cullip T J and Gabriel T A 1994 Monte Carlo study of accelerator head scatter *Med. Phys.* **21** 1383-90

Chaves A, Oliveira C, Lopes M C and Salgado J 1999 A Monte Carlo study of a linear accelerator head. Optimization of the running time to obtain the phase space source *Proc. 5th Biennial ESTRO Meeting on Physics in Clinical Radiotherapy*, ed *Radiother. Oncol.*, **51** (suppl.1):S62, Abstract 242

Deasy J O, Almond P R and McEllistrem M T 1996 Measuments of electron energy and angular distributions from clinical accelerators *Med. Phys.* **23** 675–84

DeMarco J J, Solberg T D and Smathers J B 1998 CT-based Monte Carlo simulation tool for dosimetry planning and analysis *Med. Phys.* 1–11

Deng J, Jiang S B, Kapur A, Li J, Pawkicki and Ma C-M 2000 Photon beam characterization and modelling for Monte Carlo treatment planning *Phys. Med. Biol.* **45** 411–27

Faddegon B, Balogh J, Mackenzie R and Scora D 1998 Clinical considerations of Monte Carlo for electron radiotherapy treatment planning, *Rad.Phys.and Chem.* **53** 217–27

Fragoso M, Chaves A, Alves C, Lopes M C, Oliveira C, Peralta L and Seco J 1999 MC simulation of a linear accelerator treatment head - EGS4 and MCNP-4B intercomparison' *Proc. 8th Int. Conf. on Calorimetry in High Energy Physics (Lisbon, Portugal)* ed Barreira G, Tomé B, Gomes A, Maio A and Varanda M J (Singapore:World Scientific) pp 697–702

Hartmann-Siantar C L, Chandler W P, Chadwick M B, Blann H M, Cox L J, Resler D A, Rathkopf J A, Mackie T R, Siebers J V, Ross M A, DeLuca P M Jr, Weaver K A and White R M 1995 Dose distributions calculated with the PEREGRINE all-particle Monte Carlo code (abstract) *Med. Phys.* **22** 994

ICRU 1984 Stopping powers for electrons and positrons *Report 37* (Bethesda, MD:ICRU)

ICRU 1993 Prescribing, Recording and Reporting Photon Beam Therapy *Report 50* (Bethesda, MD:ICRU)

ICRU 1999 Prescribing, Recording and Reporting Photon Beam Therapy (Supplement to ICRU Report 50) *Report 62* (Bethesda, MD:ICRU)

James F 1994 FORTRAN implementation of the high-quality pseudorandom number generator of Lüsher *Computer Phys. Commun.* **79** 111-4

Jeraj R, Keall P J and Ostwald P M 1999 Comparisons between MCNP, EGS4 and experiment for clinical electron beams *Phys. Med. Biol.* **44** 705–17

Kijewski P K, Bjarngard B E and Petti P L 1986 Monte Carlo calculations of scatter dose for small field sizes in a ^{60}Co beam *Med. Phys.* **13** 75–7

LaRiviere P D 1989 The quality of high-energy X-ray beams *Brit. Journ. Radiol.* **62** 473–81

Lee P C 1997 Monte Carlo simulations of differential beam hardening effect of a flattening filter on a therapeutic X-ray beam *Med. Phys.* **24** 1485–9

Lewis R D, Ryde S J S, Hancock D A and Evans C J 1999 An MCNP-based model of a linear acclerator X-ray beam *Phys. Med. Biol.* **44** 1219–30

Li X A and Rogers D W O 1994 Reducing electron contamination for photon beam-quality specification *Med. Phys.* **21** 791–7

Libby B, Siebers J and Mohan R 1999 Validation of Monte Carlo generated phase-space descriptions of medical linear accelerators *Med. Phys.* **26** 1476–83

Love P A, Lewis D G, Al-Affan I A M and Smith C W 1998 Comparison of EGS4 and MCNP Monte Carlo codes when calculating radiotherapy depth doses *Phys. Med. Biol.* **43** 1351–57

Lovelock D M J, Chui C S and Mohan R 1995 Monte Carlo model of photon beams used in radiation therapy *Med. Phys.* **22** 1387–94

Lüsher M 1994 A portable high-quality random number generator for lattice field theory simulations *Computer Phys. Commun.* **79** 100-10

Ma C-M, Faddegon B A, Rogers D W O and Mackie T R 1997 Accurate characterization of Monte Carlo calculated electron beams for radiotherapy *Med. Phys.* **24** 401–16

Ma C-M, Mok E, Kapur A, Pawlicki T, Findley T, Brain S, Foster K and Boyer A L 1999 Clinical implementation of Monte Carlo treatment planning system *Med. Phys.* **26** 2133–43

Mackie T R, Kubsad S S, Rogers D W O and Bielajew A F 1990 The OMEGA project: Electron dose planning using Monte Carlo simulation (abstract) *Med. Phys.* **17** 730

Mohan R, Chui C and Lidofsky L 1985 Energy and angular distributions of photon beams from medical linear accelerators *Med. Phys.* **12** 592–7

Nelson W R, Hirayama H and Rogers D W O 1985 The EGS4 Code System *Report* SLAC-265 (Standford, CA: Standford Linear Accelerator Center)

Patterson R, Daly T, Garret D, Hartmann-Siantar C, House R and May S 2000 PEREGRINE: Bringing Monte Carlo based treatment planning calculations to todays's clinic *Proc. 13th Int. Conf. on the Use of Computers in Radiation Therapy (Heidelberg, Germany)* ed Schlegal and Bortfeld (Berlim:Springer) pp 417–9

Rogers D W O and Bielajew A F 1986 Differences in electron depth-dose curves calculated with EGS and ETRAN and improved energy-range relationships *Med. Phys.* **13** 687–94

Rogers D W O, Faddegon B A, Ding C X, Ma C-M, We J and Mackie T R 1995 BEAM: a Monte Carlo code to simulate radiotherapy units *Med. Phys.* **22** 503–24

Sanchez-Doblado F, Perucha M, Leal A, Rincón M, Arráns R, Nuñez L, Rosello J, Carrasco E, Matín G, Medrano J C, Errazquin L and Sanchez-Calzado J A 2000 Computation methods for treatment verification: The full Monte Carlo contribution *Proc. 13th Int. Conf. on the Use of Computers in Radiation Therapy (Heidelberg, Germany)* ed Schlegal and Bortfeld (Berlim:Springer) pp 272–3

Siebers J V, Keall P J, Libby B and Mohan R 1999 Comparison of EGS4 and MCNP4b Monte Carlo codes for generation of photon phase space distributions for a Varian 2100C *Phys. Med. Biol.* **44** 3009–26

Siebers J V 2000 Private communication

Solberg T D, DeMarco J J, Holly F E, Smathers J B and DeSalles A A F 1998 Monte Carlo treatment planning for stereotactic radiosurgery *Rad. and Onc.* **49** 73–84

Udale M 1988 A Monte Carlo investigation of surface doses for broad electron beams *Phys. Med. Biol.* **33** 939–54